Three-dimensional strain states and crystallographic domain structures of epitaxial colossal magnetoresistive $La_{0.8}Ca_{0.2}MnO_3$ thin films

R. A. Rao, D. Lavric, T. K. Nath, and C. B. Eom[a)]
Department of Mechanical Engineering and Materials Science, Duke University, Durham, North Carolina 27708

L. Wu and F. Tsui
Department of Physics and Astronomy, University of North Carolina, Chapel Hill, North Carolina 27599

(Received 29 July 1998; accepted for publication 1 October 1998)

The evolution of three-dimensional strain states and crystallographic domain structures of epitaxial colossal magnetoresistive $La_{0.8}Ca_{0.2}MnO_3$ films have been studied as a function of film thickness and lattice mismatch with two types of (001) substrates, $SrTiO_3$ and $LaAlO_3$. In-plane and out-of-plane lattice parameters and strain states of the films were measured directly using normal and grazing incidence x-ray diffraction techniques. The unit cell volume of the films is not conserved, and it exhibits a substrate-dependent variation with film thickness. Films grown on $SrTiO_3$ substrates with thickness up to ~250 Å are strained coherently with a pure $(001)^T$ orientation normal to the surface. In contrast, films as thin as 100 Å grown on $LaAlO_3$ show partial relaxation with a $(110)^T$ texture. While thinner films have smoother surfaces and higher crystalline quality, strain relaxation in thicker films leads to mixed $(001)^T$ and $(110)^T$ textures, mosaic spread, and surface roughening. The magnetic and electrical transport properties, particularly Curie and peak resistivity temperatures, also show systematic variations with respect to film thickness. © *1998 American Institute of Physics.* [S0003-6951(98)02848-4]

Since the recent discovery of the colossal magnetoresistance (CMR) effect in epitaxial thin films of doped $LaMnO_3$,[1] there has been renewed interest in these materials for device applications.[2] The occurrence of CMR behavior has been attributed to the presence of lattice strain and disorder in epitaxial films. It has been shown[3] that the CMR effect in epitaxial $La_{1-x}Ca_xMnO_3$ (LCMO) films decreases with increasing film thickness and strain relaxation, confirming the important role of lattice strain. More recently, Suzuki *et al.*,[4] O'Donnell *et al.*,[5] and Kwon *et al.*[6] have shown that strain also plays a dominant role in magnetic anisotropy of LCMO and $La_{0.7}Sr_{0.3}MnO_3$ (LSMO) films. Millis and co-workers[7,8] have studied the effects of strain in LCMO films by measuring the out-of-plane lattice parameters and combining them with in-plane strains from calculations using Poisson's ratio, and by assuming coherence in the growth plane for films thinner than 150 Å.

In order to study the structural dependence of magnetic and electrical transport properties of these films, it is essential to characterize the structures in terms of both in-plane and out-of-plane lattice parameters. Furthermore, the thin-film unit cell volume and its distortions may not be the same as those of the bulk. Volume expansion or contraction caused by epitaxy can be stabilized by partial cation substitution[9] or oxygen nonstoichiometry. Films grown at low temperatures and low oxygen partial pressure are known[10] to be more susceptible to substrate constraints.

In this letter, we report studies of the evolution of three-dimensional (3D) strain states, crystallographic domain structures, and magnetic and transport properties of epitaxial $La_{0.8}Ca_{0.2}MnO_3$ (LCMO) films as a function of film thickness and lattice mismatch with substrates. The bulk-doped manganite LCMO is a distorted perovskite with a pseudocubic lattice parameter (a_0^P) of 3.881 Å. The tilting of the MnO_6 octahedra results in a tetragonal structure with lattice parameters $a_0^T = b_0^T \approx \sqrt{2} a_0^P$ and $c_0^T = 2a_0^P$. In this work, Miller indices used for LCMO films are based on this tetragonal unit cell, indicated by a superscript "*T*." The tetragonal distortion enables one to distinguish between the $(110)^T$-oriented films, which are equivalent to (100) or (010) in the pseudocubic perovskite unit cell, and the $(001)^T$-oriented films, which are equivalent to (001) pseudocubic perovskite, by using off-axis azimuthal (ϕ) x-ray scans, similar to what has been reported for epitaxial $SrRuO_3$ films.[11] The ability to distinguish the two tetragonal orientations is crucial for studying magnetism in these films, particularly magnetic anisotropy.

The LCMO films were grown on (001) $LaAlO_3$ ($a_0 = 3.792$ Å) and (001) $SrTiO_3$ ($a_0 = 3.905$ Å) substrates using a pulsed laser ablation technique from a stoichiometric target. The two substrates were used to provide two different types of lattice mismatch for the growth of LCMO films, -2.37% with $LaAlO_3$ (LAO) and $+0.60\%$ with $SrTiO_3$ (STO). The operating pressure was kept at 400 mTorr of oxygen with the substrate temperature held at 700 °C during deposition. The thickness of the films was varied from 100 to 4000 Å. Wavelength dispersive x-ray spectroscopy (WDS) confirmed that the composition of the films is the same as the target's within experimental error.

The 3D strain states and lattice parameters were determined by normal θ–2θ and grazing incidence x-ray diffraction (GID) θ–2θ scans. For all the films studied, the only

[a)]Electronic mail: eom@acpub.duke.edu

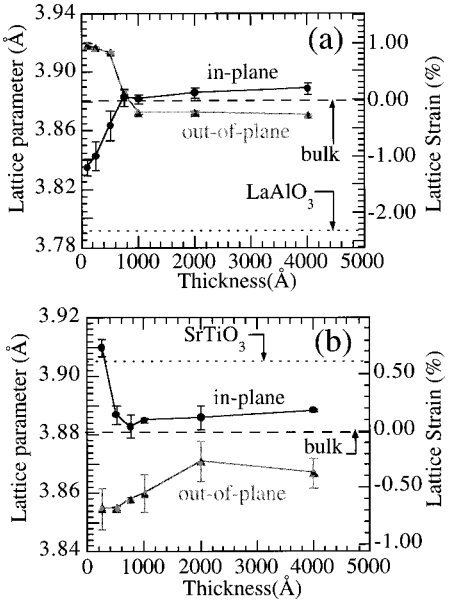

FIG. 1. Film thickness dependence of the measured out-of-plane (triangles) and in-plane (circles) lattice parameters and lattice strains of epitaxial LCMO films grown on (a) (001) $LaAlO_3$ and (b) (001) $SrTiO_3$ substrates. The lattice parameters of the bulk material measured from the target and of the substrate are indicated by the dashed lines.

intensities observed in the normal θ–2θ scans are from the substrate (001), and the film $\{001\}^T$ and/or $\{110\}^T$ reflections. We note here that GID is a surface sensitive technique, and that surface strain may not be the same as that of the bulk of the film.

The evolution of in-plane and out-of-plane lattice parameters, and the associated strains as a function of film thickness for the two different substrates are shown in Fig. 1. As expected, the observed lattice parameters for the thinnest films exhibit the largest deviations from those of the bulk, with the in-plane values at or near the substrates'. As film thickness increases, lattice relaxation takes place; both in-plane and out-of-plane lattice parameters tend to deviate away from those of the substrates towards the bulk value. The bulk values were obtained from our x-ray measurements on the target material.

The very thin LCMO films (<250 Å) grown on STO substrates are coherent, i.e., having the same in-plane lattice parameters as the substrates'. In contrast, films on LAO substrates exhibit partial strain relaxation for films as thin as 100 Å. The observed difference evidently arises from the difference in lattice mismatch between LCMO and the two substrates. It is expected that LCMO films cannot accommodate the large 2.37% biaxial compressive strain imposed by LAO and they relax even for very thin films. The strain relaxation processes are also different for growth on the two substrates. Films grown on LAO [see Fig. 1(a)] begin to relax at a very small thickness as mentioned above, and they continue to relax *gradually*. As the strains relax towards the bulk values, they undergo a sign change near 750 Å. In contrast, films grown on STO [see Fig. 1(b)] exhibit a much more abrupt relaxation in the growth plane, such that the in-plane tensile strain relaxes between 250 and 500 Å. We note that the observed behavior, particularly the sign change in strain in LCMO/LAO films, may be due to differential thermal expansion between LCMO and the substrate during sample cooling from the growth temperature. It could also be related to the oxygen stoichiometry in the films.

In order to probe the strain relaxation processes in the films, evolution of crystallographic domain structures and textures were explored. Off-axis ϕ scans of nondegenerate reflections, such as $(111)^T$, $(113)^T$, and $(221)^T$, were used to identify the specific out-of-plane orientations. From the ratio of the integrated peak intensities between the $(001)^T$ and $(110)^T$ reflections (I_{001}/I_{110}), the amount of $(001)^T$ or *c*-axis domains in the film was determined, and the values are listed in Table I as a function of film thickness for films grown on the two substrates. For very thin films grown on STO, a pure *c*-axis texture was observed. The observed in-plane epitaxial arrangement is LCMO $[110]^T$ or $[\bar{1}10]^T \| \text{STO } [100]$, and LCMO $[\bar{1}10]^T$ or $[110]^T \| \text{STO } [010]$. Very thin films grown on LAO, on the other hand, exhibit a pure $(110)^T$ out-of-plane texture with two 90° domains in plane, such that LCMO $[\bar{1}10]^T$ and $[001]^T \| \text{LAO } [100]$, and LCMO $[001]^T$ and $[\bar{1}10]^T \| \text{LAO } [010]$. As film thickness increases, the pure domain structures are replaced by mixed ones, where both $(001)^T$ and $(110)^T$ textures coexist, with the amount of mixture increasing with thickness (see Table I). This finding is consistent with previous transmission electron microscope observations.[12] The observed strain states and domain structures, as shown in Table I, exhibit strong correlation between each other, indicating that they are linked directly. For instance, the observed strain sign change in films grown on LAO appears to coincide with the 50% domain mixture, and the rapid in-plane lattice relaxation in films on STO seems to be associated with the initial appearance of $(110)^T$ textures.

Crystalline quality of the films was analyzed using the measured full width at half maximum (FWHM) of the on-axis rocking curves. For the 250 Å films, the rocking curve FWHM for the sample grown on STO is 0.25°, which is our instrument resolution, and it is between 0.25° and 0.30° for the sample on LAO, which is limited by the twinned structures of the substrate. As thickness increases, the rocking curves become broader, indicating an increased mosaic

TABLE I. Measured structural, electrical transport and magnetic data and computed Jahn–Teller and bulk strains for LCMO thin films on (001) $LaAlO_3$ and (001) $SrTiO_3$ substrates. The zero temperature resistivity intercept (ρ_0) gives an indication of the disorder in the film.

d (Å)	I_{001}/I_{110} (%)	T_p (K)	T_c (K)	ρ_0 ($\mu\Omega$ cm)	ϵ_{JT} (%)	ϵ_B (%)
			$LaAlO_3$ substrate			
4000	68	258	244	472	−0.38±0.11	0.12±0.23
2000	69	248	241	513	−0.29±0.09	0.04±0.23
1000	58	241	222	520	−0.20±0.07	−0.20±0.17
750	43	240	225	484	0.07±0.16	0.21±0.35
500	35	236	223	686	1.05±0.22	−0.06±0.53
250	0	223	203	1005	1.56±0.23	−1.06±0.54
			$SrTiO_3$ substrate			
4000	68	230	215	591	−0.45±0.03	−0.01±0.04
2000	76	212	201	605	−0.32±0.11	−0.03±0.23
1000	76	207	194	819	−0.53±0.03	−0.37±0.06
750	77	205	198	878	−0.53±0.11	−0.52±0.23
500	87	202	188	1567	−0.67±0.07	−0.39±0.17
250	100	200	188	1731	−1.16±0.11	0.79±0.21

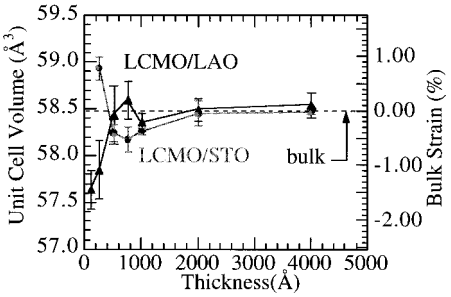

FIG. 2. Film thickness dependence of the perovskite unit cell volume and bulk strain of epitaxial LCMO films grown on (001) $LaAlO_3$ (triangles) and (001) $SrTiO_3$ (circles) substrates. The cell volume of the bulk material is indicated by the dashed line.

spread owing to the formation of the mixed $(001)^T$ and $(110)^T$ textures. For the 4000 Å films, the rocking curve FWHM is ~0.97° on LAO, and it is ~0.78° on STO substrate. Surface morphology was also studied using atomic force microscopy. While the thinner films have smoother surfaces [e.g., root mean square (RMS) roughness of ~6 Å for a 250 Å film], the thicker films are rougher (e.g., RMS roughness of ~35 Å for a 4000 Å film) due to strain relaxation.

For the LCMO system, the intrinsic strain states are the bulk strain (ϵ_B) and the Jahn–Teller (JT) strain (ϵ_{JT}), as defined in Refs. 7 and 8. The bulk strain is associated with a hydrostatic volume distortion, while the JT strain corresponds to a tetragonal distortion between the out-of-plane and in-plane lattice. These strains have been calculated using the measured lattice parameters, and they are also listed in Table I. The measured bulk strain and the associated perovskite cell volume exhibit a substrate-dependent variation with respect to film thickness, as shown in Fig. 2. For growth on either substrate, the very thin films exhibit large distortions and the thick films are structurally very similar to the bulk material. Thus perovskite unit cell volume in LCMO films is not conserved.

Temperature-dependent magnetization and resistivity of LCMO films were measured, in order to explore the effect of 3D strain states and domain structures on magnetism and transport properties. Ferromagnetic Curie temperature T_c, peak resistance temperature T_p, and zero-temperature resistivity intercept ρ_0 were obtained, and they are listed in Table I along with the structural data. The bulk pellet has a T_c of 260 K, a saturation moment of 3.64 μ_B/Mn ion, a T_p of ~260 K, and a room-temperature resistivity of 110 $\mu\Omega$ cm. Both T_c and T_p of the films increase with increasing film thickness, while ρ_0 decreases. The decreasing ρ_0 indicates a reduction of short-range disorder in the film. All measured parameters show a general trend towards bulk values at larger thicknesses. For any given film, T_c is about 10–15 K below T_p. At any given thickness, the transition temperatures for the film grown on LAO are higher than those for the STO sample. This observation is consistent with previous reports.[13,14]

While both transition temperatures and strain states exhibit strong thickness dependence as mentioned above, they do not show clear correlation with each other (see Table I). It is believed that a lattice compression (a negative ϵ_B) will reduce electron–phonon interactions and increase the electronic hopping amplitude by decreasing the Mn–O bond length while increasing the Mn–O–Mn bond angle,[15,16] all leading to a T_c increase. In contrast, the Jahn–Teller distortion will lead to a localization of electrons and reduce T_c. However, the lack of correlation between the strain states and $T_c(T_p)$ shown here suggests that the transition temperatures are also influenced by other factors, such as inhomogeneities and disorder in the film.

In summary, we have studied the evolution of 3D strain states and crystallographic domain structures of epitaxial LCMO films as a function of film thickness and lattice mismatch. We show that observed strain states exhibit a systematic, substrate-dependent change with respect to film thickness, and that the unit cell volume is not conserved. While magnetic and transport transition temperatures also show strong film thickness dependence, they do not show correlation with strain states. Certain key questions, such as the origin of the observed domain structures, strain states at the growth temperature and at T_c, and all factors that control T_c, still need to be addressed, but the 3D strain states presented here give an important first step towards elucidating the magnetic and magnetotransport properties of CMR thin films.

This work was supported by the David and Lucile Packard Fellowship (CBE), the NSF Young Investigator Award (CBE), ONR Grant No. N00014-95-1-0513, and NSF Grant No. DMR 9802444. One of the authors (F.T.) acknowledges support from NSF Grant Nos. DMR 9703419 and DMR 9601825. The authors would like to thank Dr. Jonathan Sun for helpful discussions.

[1] S. Jin, T. H. Tiefel, M. McCormack, R. A. Fastnacht, R. Ramesh, and L. H. Chen, Science **264**, 414 (1994).
[2] J. Z. Sun, W. J. Gallagher, P. R. Duncombe, L. Krusin-Elbaum, R. A. Altman, A. Gupta, Y. Lu, G. Q. Gong, and G. Xiao, Appl. Phys. Lett. **69**, 3266 (1996).
[3] S. Jin, T. H. Tiefel, M. McCormack, H. M. O'Bryan, L. H. Chen, R. Ramesh, and D. Schurig, Appl. Phys. Lett. **67**, 557 (1995).
[4] Y. Suzuki, H. Y. Hwang, S.-W. Cheong, and R. B. van Dover, Appl. Phys. Lett. **71**, 140 (1997).
[5] J. O'Donnell, M. S. Rzchowski, J. N. Eckstein, and I. Bozovic, Appl. Phys. Lett. **72**, 1775 (1998).
[6] C. Kwon, M. C. Robson, K.-C. Kim, J. Y. Gu, S. E. Lofland, S. M. Bhagat, Z. Trajanovic, M. Rajeswari, T. Venkatesan, A. R. Kratz, R. D Gomez, and R. Ramesh, J. Magn. Magn. Mater. **172**, 229 (1997).
[7] A. J. Millis, T. Darling, and A. Migliori, J. Appl. Phys. **83**, 1588 (1998).
[8] A. J. Millis, A. Goyal, M. Rajeswari, K. Ghosh, R. Shreekala, R. L. Greene, R. Ramesh, and T. Venkatesan (unpublished).
[9] R. A. Rao, Q. Gan, R. J. Cava, Y. Suzuki, S. C. Gausepohl, M. Lee, and C. B. Eom, Appl. Phys. Lett. **70**, 3035 (1997).
[10] C. B. Eom, J. Z. Sun, K. Yamamoto, A. F. Marshall, K. E. Luther, T. H. Geballe, and S. S. Laderman, Appl. Phys. Lett. **55**, 595 (1989).
[11] C. B. Eom, R. J. Cava, R. M. Fleming, J. M. Phillips, R. B. van Dover, J. H. Marshall, J. W. P. Hsu, J. J. Krajewski, and W. F. Peck, Jr., Science **258**, 1766 (1992).
[12] J. Aarts, S. Freisem, R. Hendrikx, and H. W. Zandbergen, Appl. Phys. Lett. **72**, 2975 (1998).
[13] N.-C. Yeh, R. P. Vasquez, D. A. Beam, C.-C. Fu, J. Huynh, and G. Beach, J. Phys.: Condens. Matter **9**, 3713 (1997).
[14] M. E. Hawley, C. D. Adams, P. N. Arendt, E. L. Brosha, F. H. Garzon, R. J. Houlton, M. F. Hundley, R. H. Heffner, Q. X. Jia, J. Neumeier, and X. D. Wu, J. Cryst. Growth **174**, 455 (1997).
[15] H. Y. Hwang, T. T. M. Palstra, S.-W. Cheong, and B. Batlogg, Phys. Rev. B **52**, 15046 (1995).
[16] J. M. De Teresa, M. R. Ibarra, J. Blasco, J. Garcia, C. Marquina, P. A. Algarabel, Z. Arnold, K. Kamenev, C. Ritter, and R. von Helmolt, Phys. Rev. B **54**, 1187 (1996).